Microscopic level study on the spray impingement process and characteristics

Wang, Ziman; Guo, Hengjie; Wang, Chongming; Xu, Hongming; Li, Yanfei

DOI:
10.1016/j.apenergy.2017.04.014

Document Version
Peer reviewed version

Citation for published version (Harvard):
Wang, Z, Guo, H, Wang, C, Xu, H & Li, Y 2017, 'Microscopic level study on the spray impingement process and characteristics', Applied Energy, vol. 197, pp. 114-123. https://doi.org/10.1016/j.apenergy.2017.04.014

Highlights

- Droplets splash or fingering rebound in early stages due to high velocity
- Droplets tend to stick in the end stage due to low velocity and existence of film
- Higher surface temperature affects the initial stage but not steady and end stages

Microscopic level study on the spray impingement process and characteristics

Authors: Ziman Wang[a], Hengjie Guo[b,a], Chongming Wang[a], Hongming Xu[a], Yanfei Li[b*]

[a] School of Mechanical Engineering, University of Birmingham, Birmingham, UK

[b] State Key Laboratory of Automotive Safety and Energy, Tsinghua University, Beijing 1000084, China

[*] Corresponding author. Tel: +86-10-62772515; E-mail address: liyanfei1@tsinghua.edu.cn

Abstract

Spray impingement adversely affects fuel mixture preparation, combustion performance and emissions and more studies are required to understand this process. The isooctane spray impingement process and characteristics were investigated by ultrahigh speed imaging technique with the employment of highly spatially resolved long distance microscope. The effects of impact surface temperature were also studied. It was found that during the initial stage and steady stage of spray impingement, a large proportion of droplets splashed due to high velocity. The droplet size after impingement generally reduced because of the strong collision. For the end stage of impingement, droplets tended to stick on the impact surface and float on the fuel film due to the low droplet velocity and the existence of built liquid fuel film. It was also found that hot impact surface could only improve the impingement and reduced the film building-up rate in the initial stage. The steady stage and end stage of spray impingement were less affected by the variation in impact surface temperature.

Key words: spray, impingement, breakup, film thickness

1 Introduction

The spray impingement causes fundamental issues for IC engines by altering the fuel mixing, combustion and emissions [1, 2]. If spray impingement occurs on the top of piston, the emissions due to unburn fuel are to increase [1-3]. The adverse effects of spray impingement for GDI engine are more obvious under cold start conditions where the evaporation is relatively poor due to low in-cylinder temperature. The formation of injector deposit deteriorates the influence of impingement due to the weakened atomization and prolonged penetration [4, 5]. In addition, the engine oil will be brushed away and diluted if impingement occurs on the liner wall. This will change the lubrication characteristics and the resultant piston liner friction. The mixture of fuel and engine oil also results in the oil degradation when going through high temperature. The dynamics and characteristics of the impingement process consequently become hot topics for both academy and industry.

The studies on the fundamental impact characteristics of a single droplet and multi-droplets are widely available. Five impact regimes, namely, stick, spread, splash (including prompt splash, corona splash, receding breakup, partial rebound and finger breakup), rebound and fingering were identified [2, 6]. When velocity is low, droplet would not breakup but stick on the surface, leading to the expanding and recoiling of the liquid lamella [2]. The increase of droplet velocity leads to disintegration of the periphery rim into 'fingers' and this process is governed by the impact surface roughness. Much higher velocity and inertia result in the instant disintegration of the droplet, termed 'prompt splash' [2]. Two regimes, namely, the 'splash' and 'stick-spread', are the common regimes reported for IC engines [3]. The characteristics of the secondary droplets after the impact were also investigated. It was reported that the diameter of the secondary droplet can be reduced by 90 % compared with the original droplet size if splash occurs on cold surface and that the increase of surface tension raises the size of the secondary droplets [7, 8]. For multiple-droplet impact, the impingement process is more complicated and the interaction between droplets results in different pictures compared with a single droplet impacting on surface [9]. The size of the secondary droplets from the sheet produced from interaction is larger than the size produced from single droplet impact [10, 11].

The influences of various factors on the droplets impingement also have been deeply investigated. Moita et al. [3] studied the effect of temperatures, roughness and topographies of the impact surface with the variation of wettability, viscosity and topography. It was pointed out that rougher surface promotes the droplet disintegration and that the variation of the heat transfer mechanism could affect the impingement behaviours [3, 12]. The increase of viscosity decreases the size of the crown and suppresses the secondary breakup of the droplets [3]. Some studies showed that hot surface results in a sudden rebound of droplets with low velocity after impingement due to the occurrence of vapour layer caused by the fuel evaporation at the periphery of the droplet [13, 14]. In addition, the incident angle for the impact is believed to be important since it determines the momentum transfer. Results from Mundo [12] showed that the increase of incident angle causes the increase of reflection angle and vice versa.

The abovementioned studies mainly focused on single or a few droplets. However, for real dense spray impingement in IC engines, the impact characteristics are highly dynamic due to the variation of film thickness, impact surface temperature and the resultant boundary conditions for the impingement regimes [2]. So far, few studies have been carried out to show the interaction between primary droplets and film dynamics and how secondary droplets behave under the highly transient conditions. The dynamics of the fuel film building-up are still unknown. Aiming to answer these questions, both transient and steady impact characteristics, including droplet breakup and film building-up were investigated with the employment of ultrahigh speed CCD camera and long distance microscope. The effect of impact surface temperature was also investigated.

2 Impingement theory and experimental setup

2.1 Impingement theory

The impact regimes are classified based on the characteristics of the droplets before the collision and several dimensionless parameters are used to quantify the boundary conditions. Reynolds number is used to denote the effects of inertial force and can be calculated through Equation 1.

$$\mathrm{Re} = V * d_o / \nu \tag{1}$$

Where V is the velocity, d_o is droplet diameter before the impact and ν is viscosity

Weber number is employed to denote the breakup possibility of droplets.

$$We = \frac{\rho V^2 d_i}{\sigma} \tag{2}$$

Where ρ is liquid density, d_i is critical diameter and σ is surface tension.

Moita et al. [3] defined the boundary for prompt splash and proposed the critical Weber number for the initiation of prompt splash, as shown in Equation 3.

$$Web_c = aln^b \left({}^{d_0}/_{R_a} \right) \tag{3}$$

Where a and b are coefficients, d_0 is the droplet size and R_a is the roughness of the impact surface.

Mundo [12] also defined a critical parameter, K_c, for the boundary of splash, as presented in Equation 4.

$$K_c = Oh\, Re^{1.25} \tag{4}$$

Where Oh is Ohnesorge number and can be calculated from Equation 5.

$$Oh = We^{1/2}/Re \tag{5}$$

These equations and the correspondingly calculated dimensionless numbers are used in the present study.

2.2 Experimental setup

The experimental setup mainly includes the illumination system, ultra-high speed camera together with the long distance microscope, injection system, the filter plate, the iron impact plate and heating system (not shown), as presented in Figure 1. A 500 Watt xenon lamp was employed to provide strong light which was focused by a convex lens on the target area so that the droplets at the impact surface can be clearly observed. To capture the development of the droplets during the process of impingement, an ultrahigh speed camera was used and the frame speed was set to 0.5 million, giving an interval of 2 μs between two images. The camera resolution was fixed at 312×260 pixel^2. To capture the shape of the droplets clearly, a highly-

spatially resolved long distance microscope (QM 100) was used to study the droplets behaviours in the region of 1.4 mm in height above the impact surface. The working distance of the microscope was set to 18 cm and the corresponding depth of field was around 32 μm. In addition, a magnifying lens with magnification coefficient of 2 was also used. Consequently, the resolution of the captured images is around 5.4 μm / pixel. More specifications about the imaging system can be found in [15, 16] and Table 1.

Table 1. Specification of the long distance microscope

Parameters	Information
Type	Maksutov Cassegrain Catadioptric
Working Range	15 cm to 35 cm
Resolution	1.1 microns at 15 cm
Magnification	To 34 times at image plane

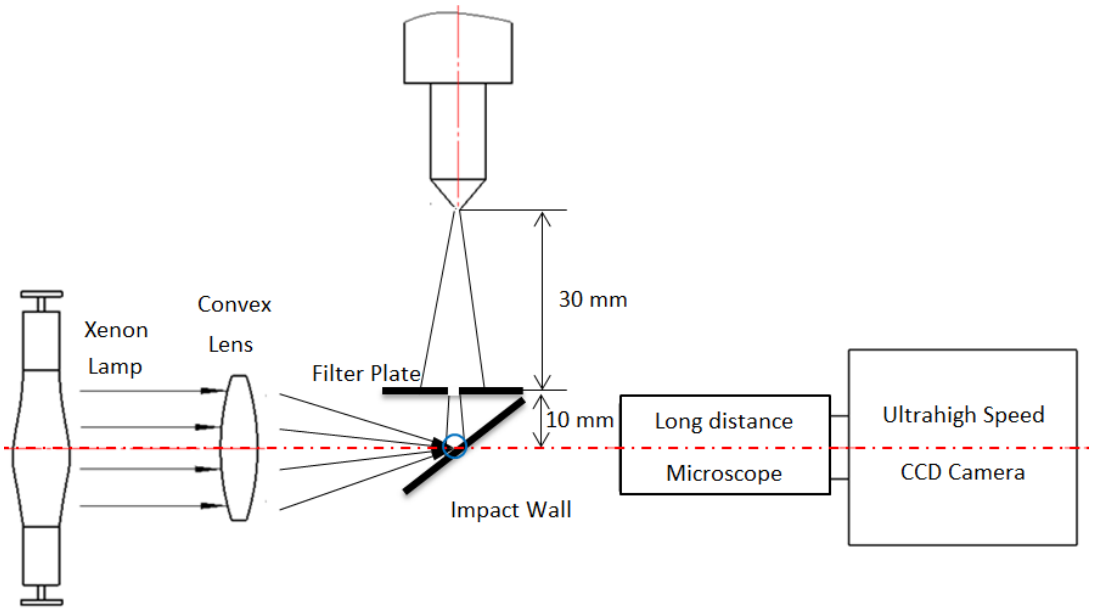

Figure 1. Experimental setup

A single hole gasoline injector with the nozzle diameter of 0.15 was used. The spray impingement occurred at 40 mm downstream of the injector and it can be expected that a large number of droplets will be seen at the collision point (the blue circle area shown in Figure 1). The appearance of numerous droplets could significantly affect the observation of the impinging process. To obtain clear images for the droplets, a filter plate was therefore used to block most of the fuel at the periphery, only allowing part of the droplets in the plume centre to pass through and impact on the surface. The hole diameter in the filter plate was 2 mm, which is believed to be sufficiently big for the view field of 1.4 mm (height) and will not affect the droplet behaviours. In addition, before every test, the filter plate was cleaned and dried to make sure that there was no fuel film built in the hole which may affect the dynamics of the droplets. The filter plate was set to 30 mm downstream of the injector tip, giving a distance of 10 mm between the impinging plate and the filter

plate. An impingement angle of 45 º was employed for all tests. A heating system consisting of 8 heaters and a close loop controller was used to heat the impact surface according to the requirements of test conditions.

3. Test fuel and conditions

Isooctane, a frequently used surrogate liquid for gasoline, was used in the present study. The properties are shown in Table 2.

Table 2. Properties of isooctane [17]

Parameter	value
Density @15 ºC (Kg/m^3)	690
Kinematic viscosity @ 40 ºC (mm^2/s)	0.72
Vaper pressure @ 21 ºC (kPa)	5.5
Surface tension @ 40 ºC (kg/s^2)	18.77 x10^{-3}
Boiling point (ºC)	99.3
Auto ignition temperature (ºC)	396

The tests were carried out under two conditions, as presented in Table 3. The cold surface condition was used as the reference and the hot surface condition was employed to study the effect of surface temperature. An injection pressure of 150 bars was used for all the tests. The roughness of the iron impact surface, Ra, is 6.3 µm. 15 repetitions were carried out for each test. The data of some figures (except the images and tables) shown in the present study are the average of the 15 repetitions. The injection duration was set to 1.5 ms. According to the spray process, three stages, namely, initial stage, steady stage and end stage were proposed. The initial stage started from the time point when the droplets were just seen in the view field. The steady stage was set to a range from 1300 µs to 1500 µs ASOI (the traveling time for the droplets from the injector tip to the impact plate was considered). As for the end stage, the timing of the camera trigger was set to 2000 µs ASOI to make sure that the last droplets with very low velocities were captured. More information for the injection stages can be found in [18, 19].

Table 3. Test conditions

Test conditions	T fuel (℃)	T impact surface (℃)	T Ambient (℃)	Ambient pressure (bar)	Impact angle (°)
Cold surface	20	20	20	1	45
Hot surface	20	160	20	1	45

4 Results and discussion

4.1 Impingement characteristics

4.1.1 Impingement during the initial stage on cold surface

Frequently observed droplet morphologies before and after impingement under 20 ºC impact surface temperature are shown in Figure 2. It should be noted that numerous droplets are involved in the impingement during the process of injection and only a few droplets travelling through the hole are studied. In this stage, 3 droplets (labelled as 1, 2 and 3) are focused when the impingement process can be clearly seen. The droplets after the impingement are labelled as 1', 2' and 3', respectively. This labelling method is applied to the rest of the present study. To make the description and explanation clear, the timing for the initial stage refers to the time after the start of collision (ASOC) because the start of impingement can be clearly identified though the imaging. However, for the steady stage and the late stage, the timing refers to the time after start of injection (ASOI). As shown in Figure 2, at the time of 0 μs ASOC, none of the three droplets collided with the surface (however other unselected droplets collided); at the time of 34 μs, droplet 1 collided; at the time of 46 μs, droplet 3 collided; at the time of 62 μs, droplet 2 collided and droplet 3 fingering rebounded; at the time of 90 μs, obvious fingering fuel columns are seen for droplets 2' and 3'. It can be seen that no big droplets /ligaments / liquid columns were seen for droplet 1 after the impingement. However, for droplets 2 and 3, obviously deformed splashed liquid columns (finger breakup) are observed. It can be expected that various impingement regimes exist in this stage, depending on the droplet velocity, diameter, fuel properties and impact surface conditions.

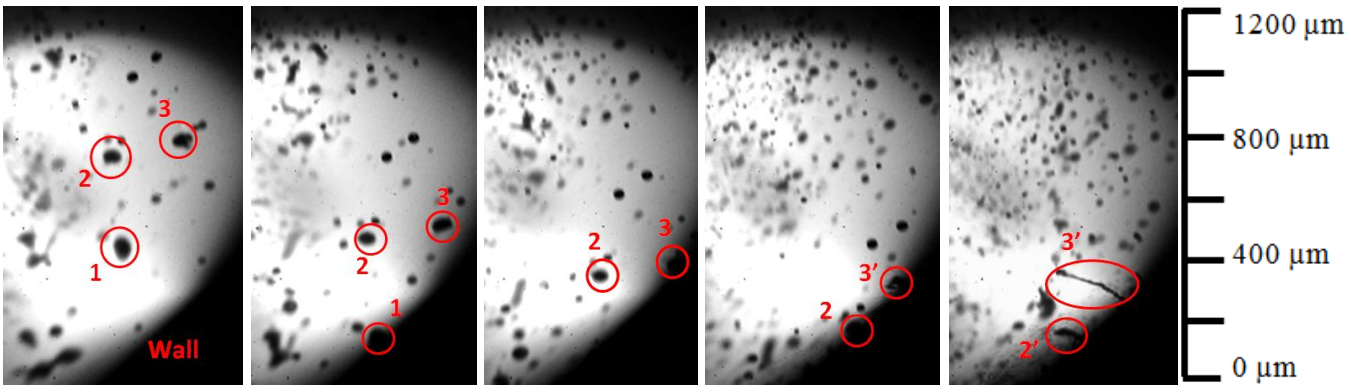

Figure 2. Droplet impingement on cold impact surface in the initial stage

Moita et al. [3] pointed out that the value of ln (R_a/d_0) is between -13 and -6 for IC engines and the results showed that the critical Weber numbers for various conditions were lower than 500 [3]. The calculated values of We in the present study shown in Table 4 are similar to the critical value and the prompt splash is expected to occur for the studied droplets. The results in the present study do not well agree with this expectation because the fingering (one type of splash) rather than prompt splash was seen in Figure 2.

In Mundo's study [12], the value of K_c for the initiation of splash was 57.7 and deposition of droplets was observed with the value of K lower than 57.7. The calculated values in the present study presented in Table 4 are all lower than the critical value and this indicates that prompt splash would not occur. This criterion applies for all 3 droplets. By comparing the critical Weber number from [3] and the critical splash number from [12] with the impingement mechanism (fingering rebound) found in the present study, it can be found that the critical splash number from Ref. 12 is more appropriate for identifying the boundary of splash mechanism. From Table 4, it can be found that the diameters of the studied droplets are larger than the SMD found in literature [4, 17] which is generally smaller than 20 μm and some reasons are responsible. The droplets are found during the initial stage (and late stage shown later) when the atomization is relatively poor and the coalescence is frequently reported [20]. More importantly, the smaller droplets are difficult to be captured by the employed imaging technique, while most of the small droplets in the literature can be detected by the PDPA. In addition, the ways of calculating the diameters are different. In the present study, the diameters of the droplets are calculated through Equation 6 shown below.

$$d = \sqrt{\frac{\bar{S}}{\pi}} = \sqrt{\frac{\int_{i=1}^{n} s_i}{n\pi}} \tag{6}$$

Where d is the mean diameter (μm), s_i is the area of droplet i in the 2D imaging plane, $\bar{S}$ is the mean area of all droplets and n is the number of droplets in the interested area.

At last, the studied droplets (shown in the tables below) are the largest ones because it is easier to quantify them through the imaging technique with a better accuracy. The application of this calculation method is due to the non-spherical shape of the droplets. It should be noted that this calculation method leads to some inaccuracy because it takes the non-spherical droplets into consideration.

Table 4. Droplet parameters before impingement on cold surface in the initial stage

Droplet	*d* (μm)	*V* (m/s)	*Re*	*We*	*Oh*	*Kc*
1	89.1	13.5	1670.6	597	6.2×10^{-4}	16.4
2	67.5	13.5	1265.6	452	7.1×10^{-4}	11.8
3	70.2	16.2	1578.4	677	6.9×10^{-4}	17.7

Table 5 Droplet parameters after impingement on cold surface in the initial stage

Droplet	*d* (μm)	*V* (m/s)	*Re*	*We*	*Oh*
2'	39	8.1	462	104.7	9.3×10^{-4}
3'	36	8.1	430	97	9.7×10^{-4}

From Figure 2 (at 90 μs after impact), it can be observed that the secondary droplets are overall smaller than the primary droplets. The potential of further breakup for the secondary droplets is also

obviously reduced after the impingement due to the decreased dynamic energy through energy dissipation and momentum transfer, as shown by the dimensionless numbers in Table 5. To study the effect of impingement on the variation of secondary droplet size, a small area just above the impact surface, 90 × 50 Pixel^2 (Figure 3), is investigated. A Matlab code was written to count the droplets in this area through the identification of the droplet boundary and calculate the mean diameter in this area. The threshold of 0.12 was employed to identify the droplet boundaries. Figure 3 (a) shows the background image which is employed as the reference background for the calculation of fuel film. Because the target area is just on the impact surface and the employed frame speed is of up to 500, 000 fps, it is extremely difficult to obtain images with identical illumination. However, the boundary of the impact surface in the background image is sufficiently clear to identify. The clear boundary allows the following calculations to be carried out. The identified boundary of the reference image (Figure 3 (a)) is shown in Figure 3 (b). It should be noted that the identification of droplets is quite accurate in the initial stages when not too many droplets are seen in the studied area. As shown in Figure 3 (c) and Figure 3 (d), the number of droplets in the original image is the same as the number of the droplets identified. However, when too many droplets are seen in this area, it is difficult to identify the droplets accurately due to the overlap of the droplet boundaries. In addition, the presence of a large amount of droplets makes it difficult to identify the fuel droplets from impact surface due to the reduced light intensity difference. In Figure 4 (a), the number of droplets is obviously larger than that in the corresponding processed area (Figure 4 (b)). The study of the influence of impingement on droplet size is therefore limited to the early stage when the droplets can be identified. It should be noted that very small droplets cannot be detected by the Matlab code. However, the results can still give some important information for the characteristics of impingement. Again, Equation 6 is used for the calculation of the droplet diameters and the sizes of the droplets are larger than those found in the literature. The results shown below are the average value of the 15 repetitions.

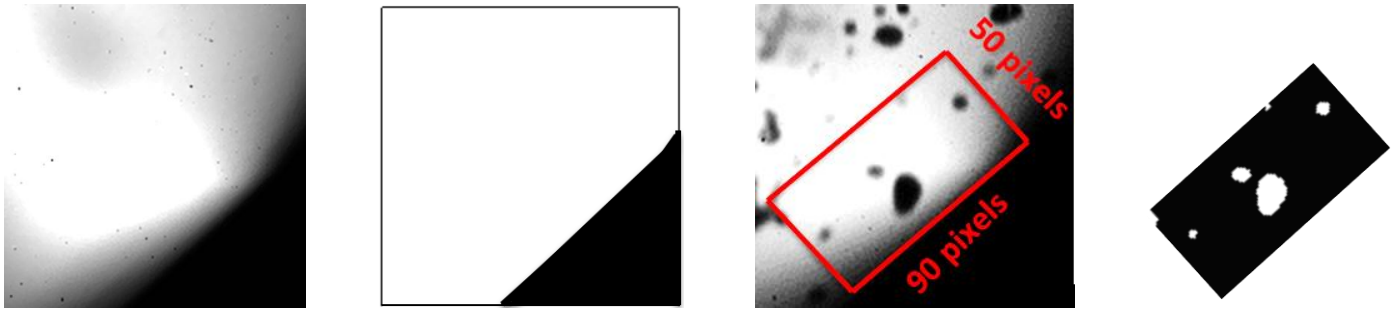

(a) (b) (c) (d)

Figure 3. Identification of droplets in the early stage, (a) background (b) processed background (c) raw image and (d) processed image

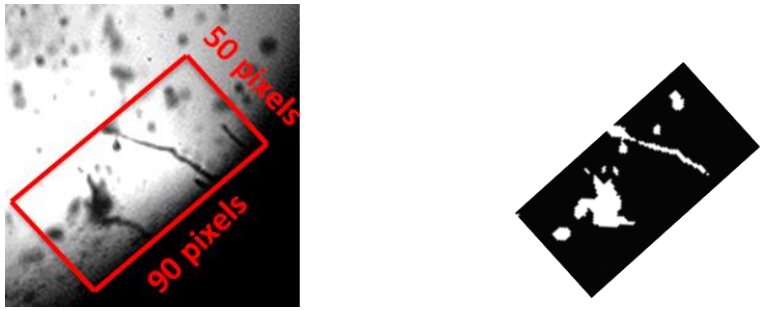

(a) (b)

Figure 4. Inaccurate identification of droplets in the initial stage, (a) raw image and (b) processed image

Figure 5 (a) shows that the mean diameter of droplets in the studied area (including primary droplets and secondary droplets) decreases until around 60 μs after impingement of the first droplet and then increases. By contrast, the corresponding number of the droplets in this area increases and then decreases. This again suggests that the occurrence of impingement reduces the droplet size, and namely the droplets after impingement are generally smaller. It should be pointed out that after 60 μs, the mean droplet size is still smaller than the size of primary droplets. However, the results in Figure 5 show the reverse trend and this is attributed to the aforementioned inaccurate boundary identification of the droplets. The existence of massive droplets, including primary droplets and secondary droplets, blurs the images and results in the failure of accurate boundary detection.

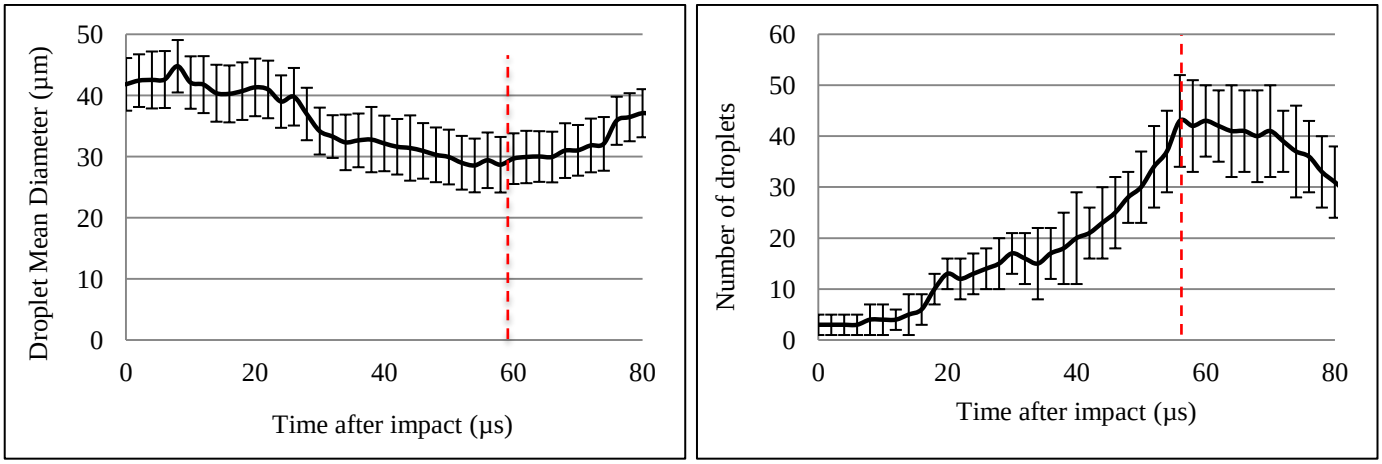

(a) (b)

Figure 5. Characteristics of impingement (a) mean droplet diameter and (b) number of droplets in the very early stage

Although the above results show that the size of droplets is reduced, the impingement actually presents adverse effect on the spray breakup and combustible mixture preparation because most of the fuel finally sticks on the impact surface, forming liquid fuel film. The fuel film building up affects both the impact boundaries and the emissions [1]. In Ref.[21], it was reported that mass fraction of deposition increases with increasing film thickness. To characterize the effect of impact on the surface wetting, the fuel film building-up is quantified in the aforementioned area (90×50 pixels^2) by another Matlab script. The calculated film building-up thickness actually includes both the liquid film and the very dense clusters due to

the rebound and splash of droplets, which are difficult to be separated from the real liquid film. Therefore, the quantified fuel film thickness should be higher than the real liquid fuel film. The calculation of the dense fuel thickness is based on boundary identification shown in Figure 3 (b). Figure 6 illustrates that the quantification of the film thickness is acceptable although some large droplets may affect the boundary identification. The film thicknesses at 3 points, the lower point (the lowest point on the impact surface in the studied area, labelled as Down), middle point (the middle point on the impact surface in the studied area, labelled as Middle) and upper point (the highest point on the impact surface in the studied area, labelled as Up), are calculated, as presented in Figure 6 (a).

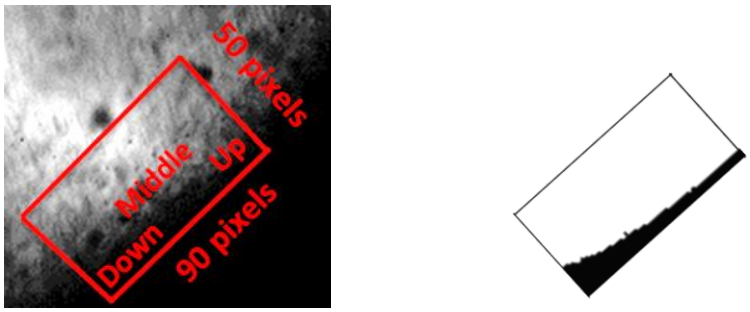

(a) (b)

Figure 6. Identification of the fuel film in the initial stage (a) raw image and (b) processed image

Figure 7 shows that the continuous impingement leads to the increase of fuel film thickness at the three points. The error bars show acceptable accuracy for the fuel film thickness and the error bars for some figures in the following sections are not shown to keep figures concise. It is interesting to find that during the first 40 μs, the film building up rates at the middle point and upper point are very slow while the film at the lower point builds up quickly. The splash or fingering rebound of the droplets during this stage leads to little fuel sticking on the impact surface. After the impact surface becomes wet, the impact regime may be altered due to the existence of liquid film on the surface and variation of droplet velocity before the impingement (this is caused by the further injector opening and resultant possible higher spray velocity). Less splashed fuel is expected to leave the impact surface due to existence of fuel film. For the ‘Down’ side, the film thickness increases consistently during the initial stage due to the fact that the liquid fuel at the upper side and middle part flowing down. It is also interesting to find that the down side shows the thickest fuel film which is obviously higher than the other two locations. The thick liquid fuel film at the down side is expected to be responsible for the significant contribution of final poor spray mixing quality.

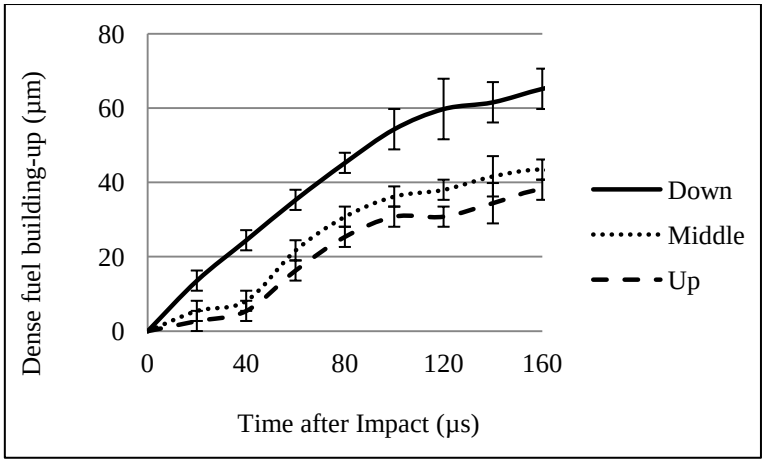

Figure 7. Dense fuel building-up on cold surface in the initial stage

4.1.2 Impingement during the steady stage on cold surface

In the steady stage, a large number of droplets and ligaments are involved. Droplets move down, collide with the impact surface and splash or fingering rebound, as presented in Figure 8. The upward splashed droplets collide with the downward droplets, causing further breakup or coalescence. Near the impact area, numerous droplets interact with each other and various collision regimes exist. The red arrows denote the moving directions of the droplets in the near region. Again it is observed that the droplets after the impingement are smaller than those before impingement and a large proportion of fuel forms a thick liquid film. It should be noted that there is an effect of strong energy dissipation upon the impact for the primary droplets because of the existence of fuel film build. The momentum of the primary droplets is quickly transferred to the liquid film upon the impact, leading to the deposition of the primary droplets. The viscosity and surface tension prevent the breakup of deposited droplets. However, very strong momentum transfer and energy dissipation can lead to the dewetting of the impact surface by lifting the liquid sheet, which results in the production of crown and small secondary droplets. Unfortunately, the existence of a large amount of primary droplets suppresses the formation of the sheet crown.

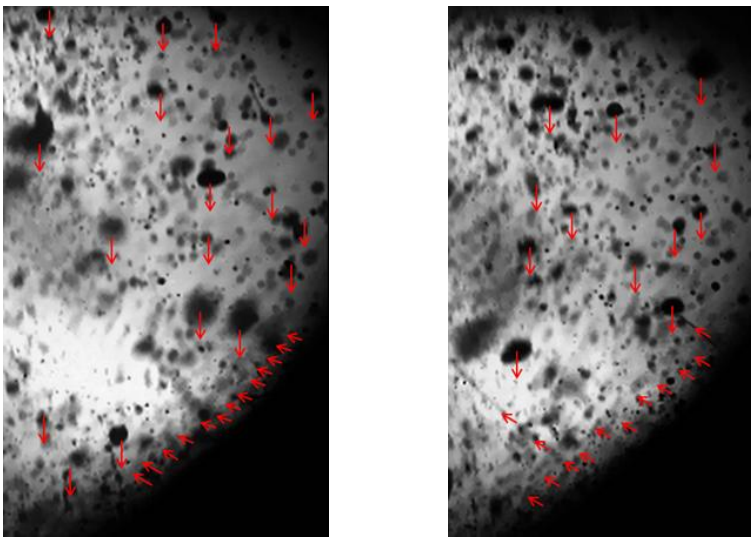

1300 μs 1306 μs

Figure 8. Droplet impingement on cold impact surface during the steady stage ASOI

The fuel film thickness in the studied region for the steady impinging stage is once again quantified, as shown in Figure 9. It can be found that the film thicknesses for these locations are quite steady with the elapse of time, suggesting that the liquid fuel flowing down along the impact surface consistently. It is interesting to find that the film thickness for the steady stage is obviously larger than that during the building-up stage (Figure 7), meaning that the building up process continues after 160 μs ASOC although the increasing rate for the fuel thickness decreases (Figure 7). In addition, the down side again shows the thickest fuel film, followed by the middle point and the upper side, suggesting that the fuel film is still considerably affected by the angle and position of impingement during the steady stage when the collision is strong and the inertial force is important.

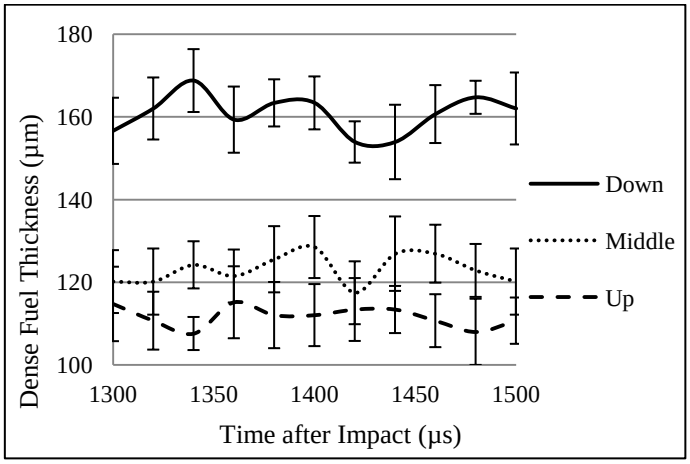

Figure 9. Dense fuel thickness on cold surface during the steady stage

4.1.3 Impingement during the late stage on cold surface

The impingement in the late stage is believed to be quite different from that in the initial or the steady stage because the droplet size tends to be large and the velocity is low. The resultant impingement is expected to be weaker and more fuel droplets are believed to stick on the impact surface. In addition, the existence of thick fuel film can considerably weaken the droplet inertia after collision. The existence of fuel film also introduces the interaction between the droplets and fuel film.

Similar to the initial stage, the impingement process for a few droplets is studied for the late stage, as shown in Figure 10. Three droplets are selected at the time of 2000 μs ASOI. At 2052 μs ASOI, droplet 1 collided with the impact surface and at 2140 μs ASOI droplet 2 impinged on the surface. The first appearances of the impinged fuel for droplets 2 and 3 are seen at 2160 μs and 2300 μs ASOI respectively. It is worth noting that droplet 1 is changed to a larger cylindrical liquid column from an almost round droplet. No splashed or rebounded small droplets are observed at the periphery. This droplet sticks on the liquid film and forms a bigger droplet with some of the liquid fuel from the film, floating down along the fuel film. However, a slightly different impingement process is found for droplets 2 and 3. Although no splashed droplets are similarly observed in the periphery, the droplets after the impingement, 2’ and 3’, are similar to the primary droplets before the impingement. The positions of the secondary droplets when observed are lower than the positions when impact. In summary, all 3 droplets stick on the fuel film and float down along

the fuel film. The droplet size after impact can increase, decrease or keep the same compared with the size of primary droplets.

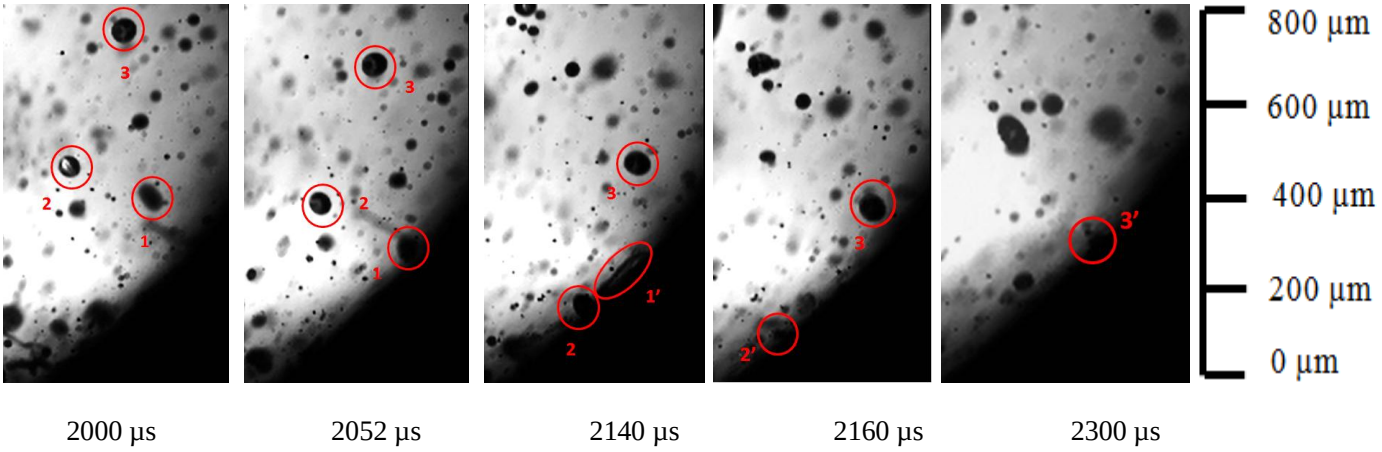

Figure 10. Droplet impingement on cold impact surface during the late stage ASOI

When compared with the impingement process for the initial stage, it can be confirmed that the impingement for the late stage is considerably weakened largely due to the low droplet velocity and partly due to the existence of the fuel film on the impinging surface. By considering the effects of liquid film, Mundo et al. [12] proposed a new way to calculate splash number, $Kc^{\#}$, as shown in Equation 7.

$$Kc^{\#} = A * Oh^{a} * We^{b} \quad (7)$$

In the study of Mundo et al. [12], the coefficients A, *a* and *b* for $Kc^{\#}$ were 1, -0.4 and 1 respectively for wet impact surface and these values are employed in the present study. The calculated parameters for the late stage are shown in Table 6. In [22], the critical splash number $K_{c,wet}{}^{\#}$ was set to $2100+5880*\delta^{1.44}$ (δ is the film thickness) for surface with fuel film where the effects of roughness can be ignored. The comparison between the calculated $Kc^{\#}$ values and the critical value $K_{c,wet}{}^{\#}$ shows that the inertias of the droplets are very low and the impingement is weak. The weakened collision (stick regime) during the late stage further deteriorates the spray mixing and emissions.

Table 6. Droplet parameters before impingement on cold surface during the end stage

Droplet	*D* (μm)	*V* (m/s)	*Re*	*We*	*Oh*	$Kc^{\#}$
1	56.7	4.05	319	34.2	7.7×10^{-4}	1.07
2	64.8	2.7	243	17.4	7.2×10^{-4}	0.6
3	70.2	2.7	263	19	6.9×10^{-4}	0.6

4.2 Effect of impact surface temperature

The evaporation of liquid fuel after impingement is expected to be affected by the temperature of the impact surface. In this section, the effects of surface temperature on the spray impingement characteristics are also investigated.

4.2.1 Impingement characteristics during the initial stage on hot surface

The morphologies of the droplet impingement are presented in Figure 11. By comparing Figure 3 and Figure 11, it can be found that background of Figure 11 is quite opaque. From Figure 11, some light gradation near the impact actually can be seen. Since the temperature of impact plate is up to 160 ºC, the temperature of the air just above the impact surface (the view field is just 1.4 mm above the surface) is believed to be quite high due to heat radiation. The high temperature of the air can significantly boost the evaporation of the droplets before the impact and the variation of gas density due to the evaporation of the droplets can also affect the light intensity and uniformity, and finally the image quality. The only thing can be observed after the impact is very small droplets (denoted by the red arrows) and opaque clusters. This is very different from the droplet morphologies for the cold case in Figure 2 where clear fingering rebound liquid columns are seen.

At 0 μs, the droplets just arrive the impact surface and begin to collide. The rest time points (32 μs, 72 μs and 108 μs) are a few points selected to check the status of the droplets after impingement. No big droplets or fingerings are observed after the collision and only a large amount of fine dispersed droplets are observed, especially at 108 μs ASOC. This is quite different from the results observed for cold impact surface. The result suggests that hot impact surface improves the impingement quality (smaller secondary droplets and less deposited liquid fuel). The possible reason is that the heat transfer from the hot surface lowers the viscosity and surface tension during the process of impingement. Consequently, the droplets tend to breakup more easily and evaporate more quickly. However, it can be expected that the effect of heat transfer is limited due to the short duration of collision. The durations for heat transfer and momentum transfer dominate the effects of surface temperature on impact process and regimes [2].

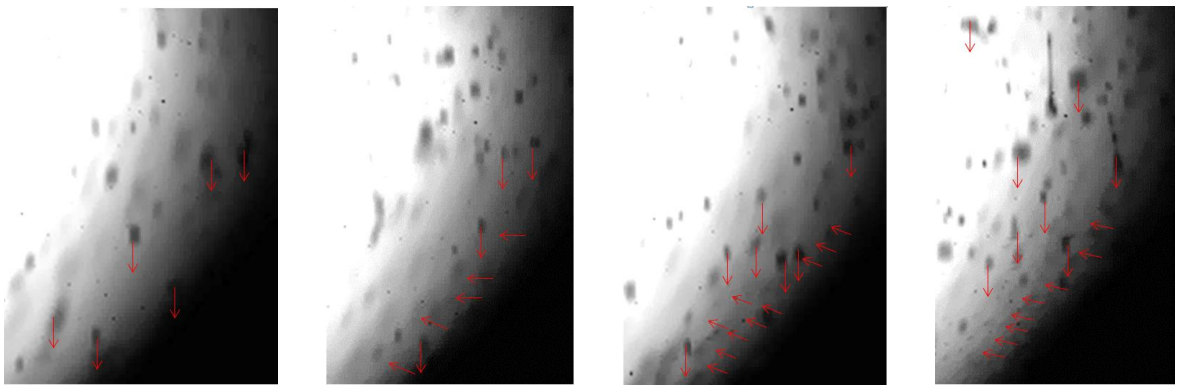

0 μs 32 μs 72 μs 108 μs

Figure 11. Droplet impingement on hot impact surface during the initial stage ASOC

The change of droplet properties after impingement in terms of size and phase (existence of liquid phase and gas phase due to the heat transfer from the impact surface) indicates that the fuel film building up process is changed because of the altered impingement regime, dispersion quality and evaporation rate from the cold case. The fuel film building up rate for the down side of the investigated area is quantified, as

illustrated in Figure 12. Higher impact surface temperature leads to slower building up rate during the initial stage. The difference is enlarged at the later stage captured in the present study.

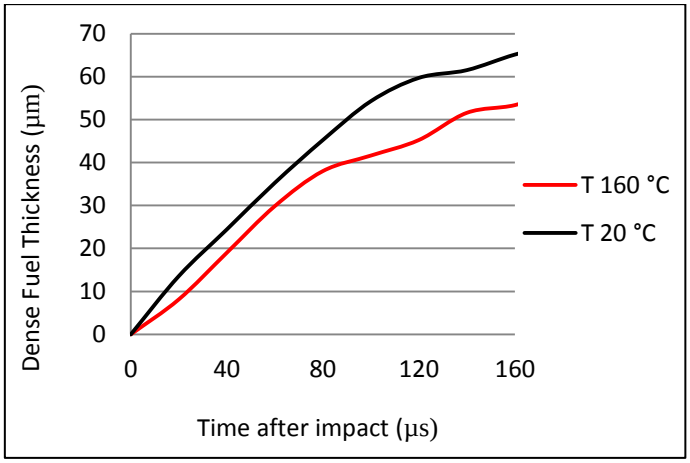

Figure 12. Influence of impact surface temperature on the film building-up

4.2.2 Impingement characteristics during the steady stage on hot surface

The morphologies of the droplets impinging on the hot surface during the steady stage are shown in Figure 13. Two timings with the difference of 64 μs are compared. A large number of small droplets are seen after the collision in the first image and some large droplets (marked by the red dotted line) are also observed after the impact in the second image. The two images show little difference of impingement when compared with that for the cold surface (Figure 8). This indicates that surface temperature (lower than 160 ºC in the present study) exerts little effects on the impingement characteristics during the steady stage. The cooling effect of the evaporation during the initial impinging stage is believed to bring down the temperature of the impact surface and no sufficient time is available for the surface temperature to recover before the steady impingement occurs. The impact surface is therefore still 'cold' for this stage and the fuel film is also built. Consequently, the boundary conditions for the impact regimes are not changed by the hot surface for this stage when compared with the cold surface case.

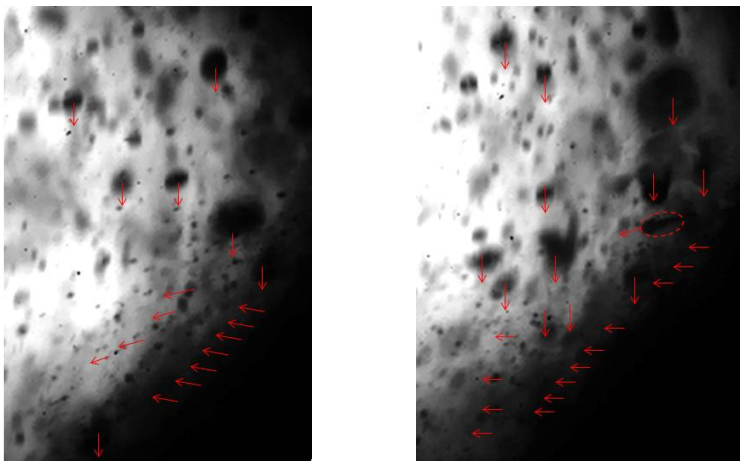

1300 μs 1364μs

Figure 13. Droplet impingement on hot impact surface during the steady stage ASOI

The comparison of film thickness for the down side during the steady stage between cold surface and hot surface again shows that the effect of surface temperature is negligible during the steady stage as little difference is observed between the two conditions (Figure 14). This suggests that the increase of surface temperature cannot alleviate the adverse effect of impingement during the steady stage.

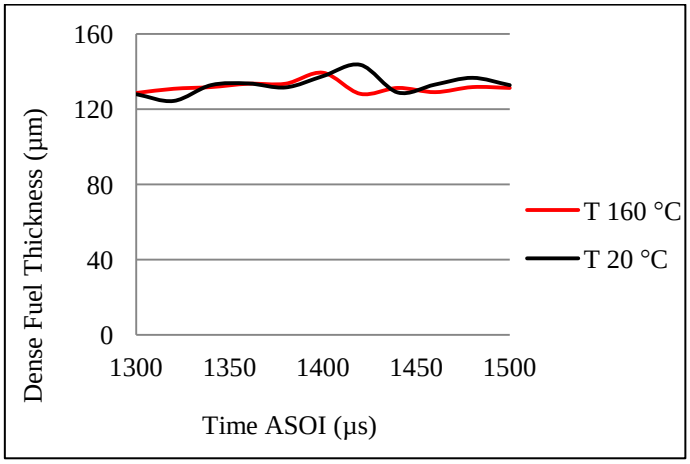

Figure 14. Influence of impact surface temperature on the film thickness

4.2.3 Impingement characteristics during the late stage on hot surface

The results for the initial stage show that hot surface boosts the fuel evaporation when the amount of impinging fuel is not very large. The impingement characteristics for the late stage may also be affected by the surface temperature because the hot surface can boost the evaporation of the fuel film built during the initial stage and steady stage. The morphologies of the two droplets for the late stage are also studied, as shown in Figure 15. The two studied droplets are at 2000 µs after start of injection when the first is to collide and 40 µs later the corresponding secondary droplet 1' is observed. After 70 µs, the second droplet collided and 100 µs later the corresponding secondary droplet was seen. For both cases, the sizes of the secondary droplets after the collision are similar to those before impact. Again, the droplets floated down along the surface and this is very similar to the results observed for cold surface. These findings suggest the impact surface temperature marginally affect the impingement characteristics for the late stage.

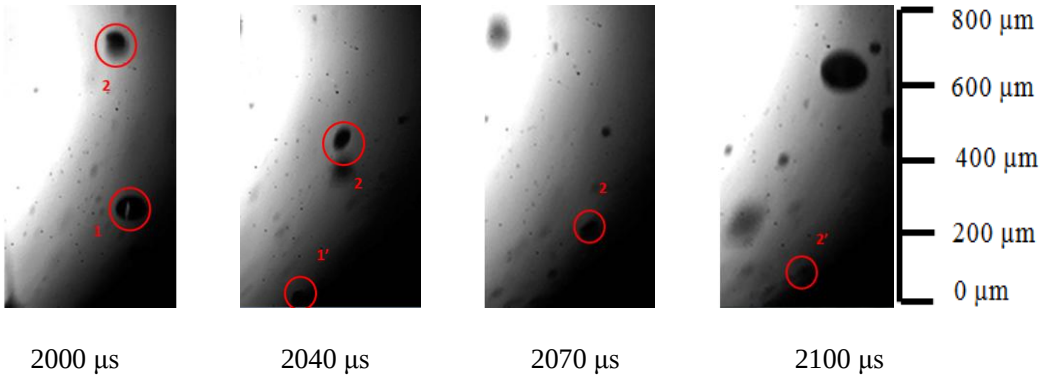

Figure 15. Droplet impingement on hot impact surface during the late stage ASOI

The dimensionless parameters for this stage are calculated and shown in Table 7. These parameters show low inertia of the droplets and thereby weak impingement. The splash numbers $Kc^{\#}$ are also much smaller than the aforementioned critical value and splash cannot happen under this condition.

Table 7. Droplet parameters before impingement on hot surface during the end stage

Droplet	D (μm)	V (m/s)	Re	We	Oh	$Kc^{\#}$
1	72	5.4	538	77	6.9×10^{-4}	2.5
2	61	5.4	457	65	7.5×10^{-4}	2.1

Conclusion

The dynamic impingement process and characterises were experimentally investigated in this study. The droplet morphologies during the impingement were captured by an ultrahigh speed CCD camera equipped with a long distance microscope. The influences of impact surface temperature on the impingement regimes and characteristics were also studied. The following conclusions can be drawn.

High velocity thereby high inertia allows droplets to fingering rebound or splash during the early and quiescent steady stages of impingement. Although the droplet sizes are reduced because of the strong collision, a large proportion of liquid fuel actually sticks on the surface, forming a fuel film, especially under low fuel temperature and low impact surface temperature condition. The very low velocity of droplets at the end stage and the existence of the liquid film on the impact surface further deteriorate the spray impingement as the droplets tend to stick and float on the film. The existence of the fuel film is expected to significantly adversely affect the spray mixing process and resultant emissions.

The impingement quality can be improved and the fuel film formation rate can be reduced in the initial stage by increasing the impact surface temperature through quicker evaporation. However, the steady stage and the end stage tend to be much less affected by the variation of surface temperature because of limited time for heat transfer during the impingement process. The evaporation rate after the impingement is believed to be higher and less liquid fuel is left on the impact wall.

Acknowledgement

This research is funded by National Natural Science Foundation of China (NSFC) under the Grant of 51636003 and China Postdoctoral Science Foundation under the Grant of 2013M540940.

Reference

[1] Cheng W.K, Hamrin D, Heywood J.B, Hochgreb S, Min K, Norris M, An overview of hydrocarbon emissions mechanisms in spark-ignition engines, SAE Tech Paper, 1993, 932708.

[2] Moreira A.L.N, Moita A.S, Panao M.R, Advances and challenges in explaining fuel spray impingement: How much of single droplet impact research is useful? Progress in Energy and Combustion Science, 36 (2010) 554-580.

[3] Moita A.S, Moreira A.L.N, Drop impacts onto cold and heated rigid surfaces: morphological comparisons, disintegration limits and secondary atomization. Int J Heat Fluid Flow 2007, 28(4):735-72.

[4] Wang Z.M, Ma X, Jiang Y.Z, Li Y.F, Xu H.M. Influence of deposit on spray behaviour under flash boiling condition with the application of closely coupled split injection strategy. Fuel, Volume 190, 15 February 2017, Pages 67-78.

[5] Xu H, Wang C.M, Ma X, Sarangi A.K, Weall A, Krueger-Venus J, Fuel injector deposits in direct-injection spark-ignition engines. Progress in Energy and Combustion Science. 2015; 50:63-80,

[6] Rioboo R, Tropea C, Marengo M, Outcome from a drop impact on solid surfaces. Atom Sprays 2001; 11:155-65.

[7] Levin. Z, HOBBS. P. V, Splashing of drops on solid and wetted surfaces: hydrodynamics and charge separation. Phil. R. Soc. Lond. 1971, A 269, 555-585.

[8] Stow C. D, Hadfield M. G, An experimental investigation of fluid flow resulting from the impact of a water drop with an unyielding dry surface. Proc. R. Soc. Lond. 1981, A 373, 419-441.

[9] Roisman I.V, Horvat K, Tropea C, Spray impact: rim transverse instability initiating fingering and splash: description of a secondary spray. Phys Fluids 2006, 18:102104.

[10] Cossali G.E, Marengo M, Santini M. Impact of single and multiple drop array on a liquid film. In: Proc 19th ILASS-Europe, Nottingham, UK; 2004.

[11] Cossali G.E, Marengo M, Santini M. Drop array impacts on heated surfaces: secondary atomization characteristics. In: Proc 19th ILASS-Europe, Notting ham, UK; 2004.

[12] Mundo C.H.R, Sommerfeld M, Tropea C. Droplet-wall Collisions: experimental studies of the deformation and break-up processes. Int J Multi Flow 1995; 21(2):151-73.

[13] Wachters H. J, Westerling N. A.J, The heat transfer from a hot wall to impinging water drops in a spherical state. Chem. Ing. Sci. 21, 1963, 1047-1056.

[14] Anders K., Roth N, Frohn A. 1993 The velocity change of ethanol droplets during collision with a wall analysed by image processing. Exp. Fluids 15, 91-96.

[15] Wang Z.M, Ding H.C, Ma X, Xu H.M, Wyszynski M.L, Ultra-high Speed Imaging Study of the Diesel Spray Close to the Injector Tip at the Initial Opening Stage with Single Injection. Applied Energy, Volume 165, 1 March 2016, Pages 335-344.

[16] Wang Z.M, Li Y.F, Xu H.M, Wyszynski M.L, Experimental study on primary breakup of diesel spray under cold start conditions. Fuel, Volume 183, 1 November 2016, Pages 617-626.

[17] Wigley G, Mojtabi M, Williams M, Pitcher G, The Effect of Fuel Properties on Liquid Breakup and Atomization in GDI Sprays, ICLASS06-075, 2006.

[18] Wang Z.M, Wyszynski M.L, Xu H.M, Abdullah N.R, Piaszyk J, Fuel injection and combustion study by the combination of mass flow rate and heat release rate with single and multiple injection strategies. Fuel Processing Technology. Volume 132, April 2015, Pages 118-132.

[19] Wang Z.M, Ding H.C, Wyszynski M.L, Tian J.Y, Xu H.M, Experimental study on diesel fuel injection characteristics under cold start conditions with single and split injection strategies. Fuel Processing Technology. Volume 131, March 2015, Pages 213-222.

[20] Wang Z.M, Jiang C.Z, Xu H.M, Wyszynski M.L. Macroscopic and microscopic characterization of diesel spray under room temperature and low temperature with split injection. Fuel Processing Technology 142 (2016) 71-85.

[21] Samenfink W, Elsaber A, Dullenkopf K, Wittig S, Droplet interaction with shear-driven liquid films: analysis of deposition and secondary droplet characteristics. IntJ Heat Fluid Flow1999; 20:462-9.

[22] Cossali G.E, Coghe A, Marengo M, The impact of a single drop on a wetted solid surface. Exp Fluids 1997, 22:463-72.